Supporting Information

De novo design, solution characterization, and crystallographic structure of an abiological Mn-porphyrin binding protein capable of stabilizing a Mn(V) species

Samuel I. Mann[‡], Animesh Nayak[§], George T. Gassner[‖], Michael J. Therien[§], William F. DeGrado*[,‡]

[‡]Department of Pharmaceutical Chemistry and the Cardiovascular Research Institute, University of California at San Francisco, San Francisco, California 94158-9001, United States

[§]Department of Chemistry, Duke University, Durham, NC 27708

[‖]Department of Chemistry and Biochemistry, San Francisco State University, San Francisco, California 94132, USA.

Contents

Methods

MPP1 Design Process. The design of MPP1 began with the parameterized backbone of the 4-helix bundle, PS1.[1] Like PS1, MPP1 utilized an axial His ligand and second-shell H-bonded Thr residue in the *d* and *b* positions of the heptad repeat, respectively, to bind the abiological porphyrin, $[Mn^{III}DPP]^+$, with a dioxygen unit bound in the open coordination site (trans to the axial His ligand). The cofactor was placed by hand, orienting the appended phenyl rings to sit down the long axis of the bundle. Due to the size of the cofactor relative to the Zn-porphyrin used in PS1, the protein was extended by ten residues. The remaining cofactor-free region of the protein was designated as the "folded core". Because PS1 was soluble and expressed well in *E. coli*, we chose to retain the majority of the surface residues while computationally designing the interior residues in the binding site and folded core simultaneously. A flexible backbone sequence design protocol was used (see below) to design the parameterized backbone sequence and packing around the MnDPP(OOH) cofactor. Note that residue numbering here and in the main text is consistent with expressed MPP1, which contains a N-terminal 6xHis tag and TEV protease cleavage site.

Loop Design. Loops were selected using MASTER (Method of Accelerated Search for Tertiary Ensemble Representatives)[2]. Segments of adjacent helices (6 residues from each helix) were queried against a database of structures from the PDB. Using the "wgap" option in MASTER, loops of specified length connecting these helices were found within a given rmsd cutoff. These loops were then clustered on rmsd and scored based on number of outputs in a given cluster. Loops were chosen from well-populated clusters (Table S1). LoopAB and loopCD are two residues and constrained in the residue file to a Gly-Asp motif. This ensured favorable N-capping and C-capping interactions to support the folded core.[3-4] LoopBC had a lower representation than loopAB/CD but a large cluster was found nonetheless.

Table S1. Results from clustering loops output from MASTER for MPP1.

Loop	Number loops in cluster (<1 Å)	Average r.m.s.d. (Å)	Loop Motif
AB	200	0.34 ± 0.03	$\alpha_L\beta$
BC	83	0.85 ± 0.1	$\alpha_L\beta\beta\beta\beta$
CD	200	0.27 ± 0.03	$\alpha_L\beta$

Flexible Backbone Sequence Design. We wrote a RosettaScript for flexible backbone sequence design, implemented in Rosetta 3.5, that progresses through a cycle of backbone and side-chain relaxation and fixed backbone sequence design, with a filtering step based on packing score (see RosettaScript below).

Amino acids allowed to vary during design. To avoid deleterious oxidations within the active site we disallowed Tyr and Trp residues within 10 Å of the cofactor and disallowed Cys and Met residues throughout the protein. Additionally, no His residues were allowed except for the axial His ligand. The residue files (resfile_ex1.txt, resfile_ex3.txt, resfile_aro.txt) are provided below showing exactly which residues were allowed to be designed. All 64 interior residues (except Thr27 and His64, which are keystone interactions for Mn binding) and loopBC were allowed to vary during design. Ultimately, 65% of the interior residues changed (relative to PS1) with the majority occurring in the binding site to accommodate the new cofactor (Fig. 2).

Flexible backbone design protocol. Distance and angle constraints (constraints.cst) between His and Mn and Thr and His were loaded, the sequence was designed with a fixed backbone, the sidechains and backbone were minimized, three trials of a Monte Carlo flexible backbone subprotocol were performed followed by one trial of an additional Monte Carlo flexible backbone protocol with additional rotamers allowed, and 100 models with packing score (pstat) > 0.48 were output. Designs were visualized with PyMol and analyzed for total score and pstat to choose MPP1.

Flexible backbone design sub-protocol. The flexible backbone design sub-protocol consists of three Monte Carlo trials of (1) fixed backbone design with ref2015 weights and the addition of extra rotamer sampling around χ_1 (ex1, level 1; i.e. sampled between 1 standard deviation of the mean chi angle value for reach rotamer) and χ_2 (ex2, level 1) sidechain dihedrals, (2) fast relax minimization (with increased repulsive features from rosettacon2018 modifications). At the end of step (2), the model is filtered for native-like structure packing with PackStat (if 1 of 3 trials the PackStat score is > 0.48 the model passes the filter). This model then undergoes an additional Monte Carlo trial of (1) fixed backbone design as above, but with rotamers sampled between 2 full standard deviations of the mean chi angle (ex1, level 3) and sidechain dihedrals (ex2, level 3), (2) rosettacon2018-modified FastRelax, and (3) a final PackStat filter required pstat > 0.48. The final designed sequences of MPP1-4 selected for expression were as follows:

>MPP1
SEKEELFEKLKQTADEAVQLFQRLREIFDKGDDDSFEQVLEELEEALQKHRQLADQGRK
KGLLTSEAAKQGDQFVQLFQRFREAWDKGDKDSLEQILEELEQVAQKAVELGLKILKT
Q

>MPP2
SEEIARKILEKLKQTADEAVQLFQRLREIFDKGDDDSFEQVLEELEEALQKHRQLADQGV
KKGGLGSDEALKQGDQFLQLFQRFREAWDKGDKDSLEQILEELEQVAQKAVELGLLKA
ELT

>MPP3
AGELIAIAAEKLKQTADEAVQIFQRLREIFDKGDDDSWEQVAEELEEALQKHRQIAENIV
KKFEEGLKATRDLVIKQGDQFLILWQRYREAWDKGDKDSLEQILEELEQVAQKAVELG
LKAARSD

>MPP4
SEIEKLKQTADEAVQIFQRLREIFDKGDDDSFEQVAEEFEEALQKHRQLYDNRPEGFGTE
VAKQGDQFVQLWQRFREAWDKGDKDSLEQILEELEQVAQKAVELGLKKN

Ab initio folding. Rosetta *ab initio* folding prediction calculations[5] were performed on the MPP1 sequence in Rosetta 3.5. 10,000 structures were generated. Cα RMSD of the folded core was scored against residues 4-29, 34-59, 66-86, and 91-115 of the design model. Cα RMSD of the binding region was scored against residues 3-20, 47-59, 66-75, and 103-116 of the design model. Cα RMSD of the folded core region was scored against residues 21-29, 34-46, 76-86, and 91-102 of the design model (Fig. S2).

Size exclusion chromatography. Gel filtration profiles were obtained using a Superdex 200 10/300 column on an FPLC system (GE Healthcare AKTA). 500 µL of 500 µM apo-MPP1 or 400 µM holo-MPP1 was injected onto the column and eluted with a 50 mM MES, 150 mM NaCl, pH 7.5 buffer mobile phase at a flow rate of 0.3mL/min.

Circular dichroism (CD). CD spectra were collected on a Jasco J-810 CD spectrometer in a 0.1 cm path length quartz cuvette, using temperature/wavelength mode. Spectra were collected from 20 to 90 °C with an interval of 5 °C and an increase rate of 2 °C/minute, over a wavelength range from 200 to 250 nm. Apo- and holo-MPP1 were prepared at 9.6 µM and 3.8 µM, respectively, for 200-250 nm window and 375 µM for the visible region in 50 mM MES, 150 mM NaCl pH 7.5.

Electronic absorption spectroscopy. Electronic absorption spectra were collected using an HP 8453 UV-Vis spectrophotometer or Cary 300 Bio spectrophotometer in a low-volume (750 µL) 1-cm path-length quartz cuvette.

Visualization of protein structures and image rendering. Protein models were visualized and rendered in the PyMol visualization program.[6]

Protein expression and purification. The gene coding for the protein sequence of MPP1 was ordered from IDT, which was cloned into the IPTG-inducible pET-21a plasmid (cloning site NdeI-BamHI). The sequence also coded for an N-terminal 6xHis-tag followed by a TEV protease cleavage sequence, followed finally by the designed sequence. The cloned gene sequence is:
ATGCATCACCACCACCACCACGAGAACCTGTACTTCCAAAGCAGCGAGAAAGAGGA
GCTGTTTGAAAAGCTGAAACAGACCGCGGATGAGGCGGTGCAGCTGTTCCAACGTC
TGCGTGAAATCTTTGACAAGGGTGACGATGACAGCTTCGAACAGGTTCTGGAGGAA
CTGGAGGAAGCGCTGCAGAAACACCGTCAACTGGCGGATCAGGGTCGTAAGAAAGG
CCTGCTGACCAGCGAGGCGGCGAAGCAGGGTGATCAATTTGTTCAACTGTTCCAACG
TTTTCGTGAAGCGTGGGACAAGGGCGATAAAGACAGCCTGGAGCAAATCCTGGAGG
AACTGGAACAGGTGGCGCAAAAAGCGGTTGAGCTGGGCCTGAAGATTCTGAAAACC
CAG

The expressed protein sequence was finally:
MHHHHHHENLYFQ/SSEKEELFEKLKQTADEAVQLFQRLREIFDKGDDDSFEQVLEELEE
ALQKHRQLADQGRKKGLLTSEAAKQGDQFVQLFQRFREAWDKGDKDSLEQILEELEQV
AQKAVELGLKILKTQ

where the "/" defines the cleavage site of TEV protease. The plasmids were transfected into *E. coli* BL21(DE3) cells, which were grown in LB/carbenicillin media until OD @ 600 nm = 0.6. The cells were then induced with 1 mM IPTG (final concentration) and allowed to grow for 4 more hours. Cells were then centrifuged and frozen. The frozen cell pellets were lysed via sonication in 50 mM MES, 150 mM NaCl, 20 mM imidazole pH 7.5. The expressed, His-tagged MPP1 protein was purified via a Ni NTA column (Fisher) and confirmed by gel electrophoresis, with an approximate yield of 25 mg/L. MPP2-4 were expressed and purified in the same manner.

NMR spectroscopy. All NMR samples contained 0.2 mM protein in a 50 mM phosphate buffer at pH 7.5 and 5% D_2O. 1D Spectra were recorded at 298 K on a Bruker 800 MHz spectrometer equipped with a cryogenic probe. The ^1H zgesgp spectra were recorded with 512 scans with 30 ppm spectral width. ^1H chemical shifts were referenced with respect to the residual water peak at 4.75 ppm. All spectra were processed and analyzed using the program TopSpin 3.6 (Bruker, Karlsruhe, Germany). Prior to Fourier transformation, time domain data were multiplied by sine square bell window functions shifted by 90º and zero-filled once.

Oxidation with $NaIO_4$ and sulfoxidation of thioanisole. To a 1 mL solution of 10 µM Mn(III)MPP1 in 50 mM MES, 150 mM NaCl pH 7.5 in a quartz cuvette, 100 µL of 100 mM $NaIO_4$ stock solution in water was added. The reaction was monitored with 30 s scans until the absorbance at 430 nm reached its maximum. Then 1 µL of a 100 mM thioanisole stock solution in DMSO was added and mixed by hand before recording spectra every 3 s. The reaction was completed after ~ 1 minute and the reaction mixture was directly injected on the mass spectrometer for analysis. Performing the control reaction with thioanisole and $NaIO_4$ showed no evidence of sulfoxidation in the mass spectrum. These reactions were also performed in buffer containing 50 mM sodium phosphate, 150 mM NaCl pH 7.5 with no observable difference as compared to the MES buffer condition.

Equilibrium spectrochemical redox titrations.[7] To a 2 mL solution of 15µM Mn(III)MPP1 in 50 mM phosphate, 150 mM NaCl pH 7 buffer, a redox indicator dye (Indigo-5-5'-disulfonic acid, IDIS, with midpoint reduction potential at neutral pH, $E_{m,7}$ = −125 mV versus SHE) was added to a 28 µM concentration. The sample was then transferred to an anaerobic quartz cuvette and degassed by sequential vacuum pumping and purging with N_2. The quartz chamber was fitted with a 250 µl Hamilton Gastight syringe containing degassed 2.16 mM sodium dithionite solution. After an initial spectrum collection, a 5 µl aliquot of the dithionite solution was injected with reduction occurring within the mixing time. Dithionite was added in increments of 5 µl until the Mn(III) Soret at 463 nm had converted to the Mn(II) Soret at 430 nm. The ratio of corresponding oxidized and reduced species present after each addition of dithionite was computed after spectral deconvolution of the absorbance spectra recorded in the titration. This was done by using basis spectra of the oxidized and reduced forms of the protein and indicator. The equilibrium midpoint potential of MPP1 was computed with equation (1) which uses the known midpoint potential of the redox indicator as a reference point (Fig. S13). This process was repeated with the redox indicator dye (potassium indigotrisulfonate, ITRIS, with $E_{m,7}$ = -81 mV vs SHE). The potential values obtained from each dye were averaged to give -107 mV vs SHE and the error (± 5 mV) was calculated from the standard deviation of the two potentials.

$$E_m^{ref} - \frac{RT}{nF} ln \frac{[Dye_{red}]}{[Dye_{ox}]} = E_m^{Mn(^{III}/_{II})} - \frac{RT}{nF} ln \frac{[Mn^{II}]}{[Mn^{III}]} \qquad \textit{(1)}$$

Equilibrium spectroelectrochemical experiments. The spectroelectrochemical experiments were done using Honeycomb Spectroelectrochemical Cell Kit (Pine Instruments) in a quartz cuvette (1.7 mm path length) using a gold surface as working and counter electrodes and Ag/AgCl as reference electrode (values were converted to SHE for comparison). Indigo-5,5′-

disulfonic acid disodium salt (50-100 μM) was added as redox mediator in the protein solution (~5-10 μM) in phosphate buffer (50 mM with 150 mM added NaCl). After degassing by vacuum purging with argon for at least 12 cycles, electrolysis of the solution was performed by holding the potential of the working electrode until the spectral change was complete (15-20 min). Electrolysis potential ranging from -200 mV to -600 mV vs Ag/AgCl (10 to -390 mV vs SHE) was changed by increments of 25-50 mV. Spectroelectrochemical changes of redox mediator was recorded under same electrolysis potential and the absorption for the redox mediator was subtracted from the original spectra to obtain spectra of the protein (Fig. 5). From the spectral changes at 430 nm (corresponding to Mn(II)) and 460 nm (corresponding to Mn(III)), percent conversion was calculated and plotted versus applied potential. Midpoint potential was found from the plot at 50% conversion. The same procedure was performed at pH ranging from pH 6 - pH 8; these midpoint potential values are listed in Table S2. Attempts to measure the potential at pH < 6 were complicated by possible protonation of the axial His ligand.

Crystallization of MPP1. A solution of holo-MPP1 was concentrated via centrifugation in an Amicon Ultra – 0.5 mL centrifuge filter (10 kDa MW cutoff) until a concentration of 60 mg/mL was reached (based on measured absorbance at 463 nm, ε_{463} = 65,000 M^{-1} cm^{-1}). Crystallization conditions were screened against the Hampton Crystal HT matrix with a Mosquito Crystal instrument. Crystals were found with the following conditions: a 0.2 μL hanging-drop (0.1 μL holo-MPP1 and 0.1 μL crystallization buffer (0.1 M HEPES pH 7.5, 0.8 M NaH_2PO_4, 0.8 M KH_2PO_4)). Crystals were harvested, cryo-protected in 30% glycerol in crystallization buffer for 30 seconds before being flash-frozen in liquid nitrogen.

MPP2 was screened against 3 crystallization matrices (Hampton Crystal HT, Index, and SaltRx 1 and 2) but no crystals were obtained.

Data collection and processing. Diffraction data was collected at SSRL Beamline 12-2 on a PILATUS 6M detector with a 1.11 Å wavelength at 100 K. Data were processed with HKL2000[8] and statistics for data processing and structural refinement can be found in Table S3. The structure was solved by molecular replacement with Phaser[9] using the MPP1 design model. Phenix was used for refinement and REEL was used for ligand manipulation. Cofactor placement was based on residual electron in the binding site along with anomalous maps phased from metal ion-free models after molecular replacement. Additional density on the surface of the bundle near E58 was found and modelled as an additional MnDPP. It sits on a C2 symmetry axis and was therefore modelled with 50% occupancy. In solution, the protein is monomeric and binds a single equivalent of MnDPP cofactor (Fig. 3B). Therefore, this is likely a crystallographic artifact. Protein model building and adjustments were performed in Coot.[10]

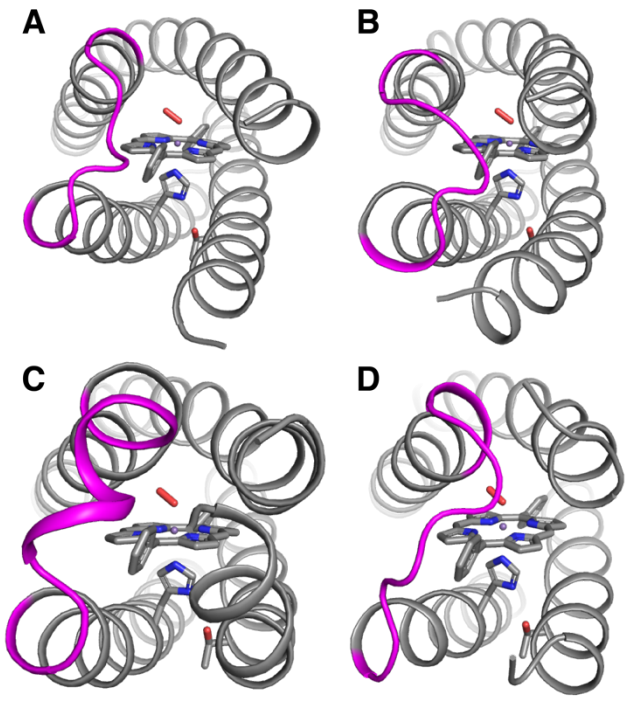

Figure S1. Rosetta models of MPP1 (**A**), MPP2 (**B**), MPP3 (**C**), and MPP4 (**D**) highlighting the different loops chosen (purple) using MASTER.

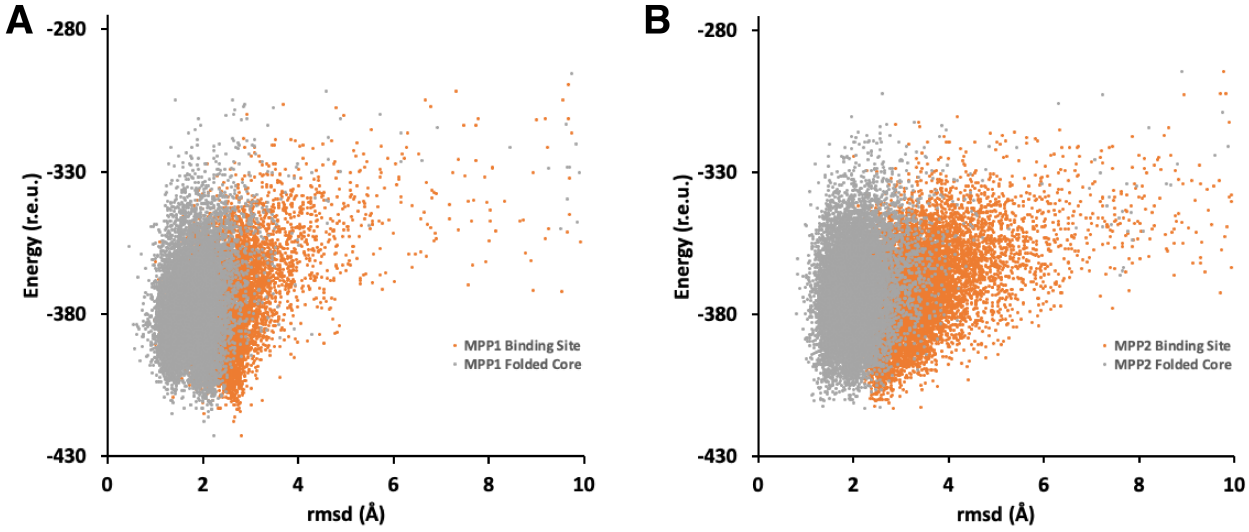

Figure S2. Rosetta *ab initio* folding predictions for (**A**) MPP1 and (**B**) MPP2 comparing the binding site and folded core. The folding algorithm predicts a lower RMSD for the folded core region (grey) versus the binding site region (orange) of apo-MPP1 and apo-MPP2.

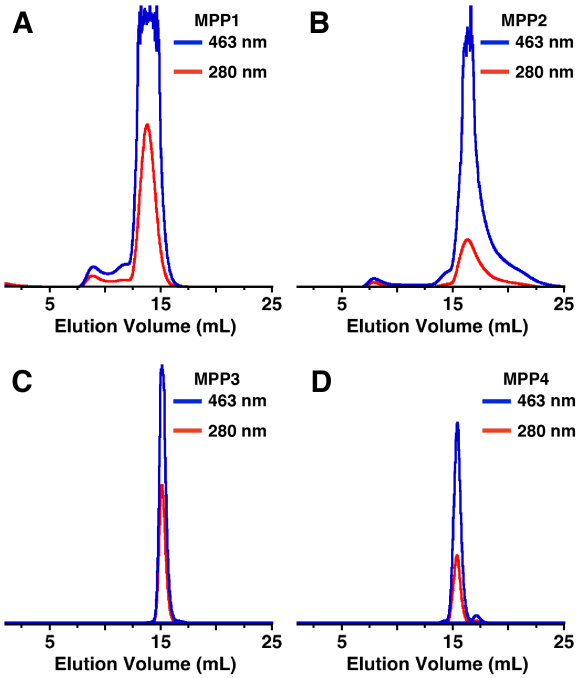

Figure S3. FPLC traces showing that holo-MPP1(**A**), holo-MPP2 (**B**), holo-MPP3 (**C**), and holo-MPP4 (**D**) are monomers in solution and elute with the MnDPP cofactor (based on the absorbance at 463 nm).

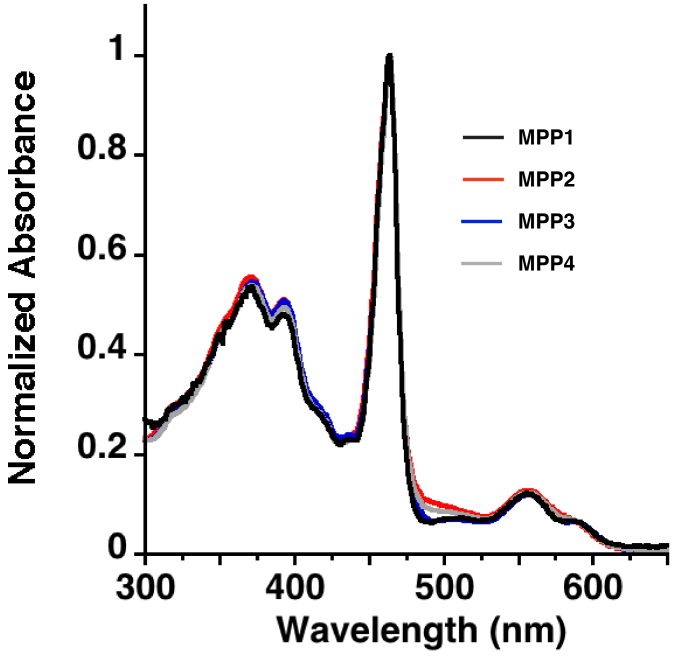

Figure S4. Electronic absorption spectra of holo-MPP1-4 showing identical spectral features suggesting similar binding environments for the Mn(III)DPP cofactor.

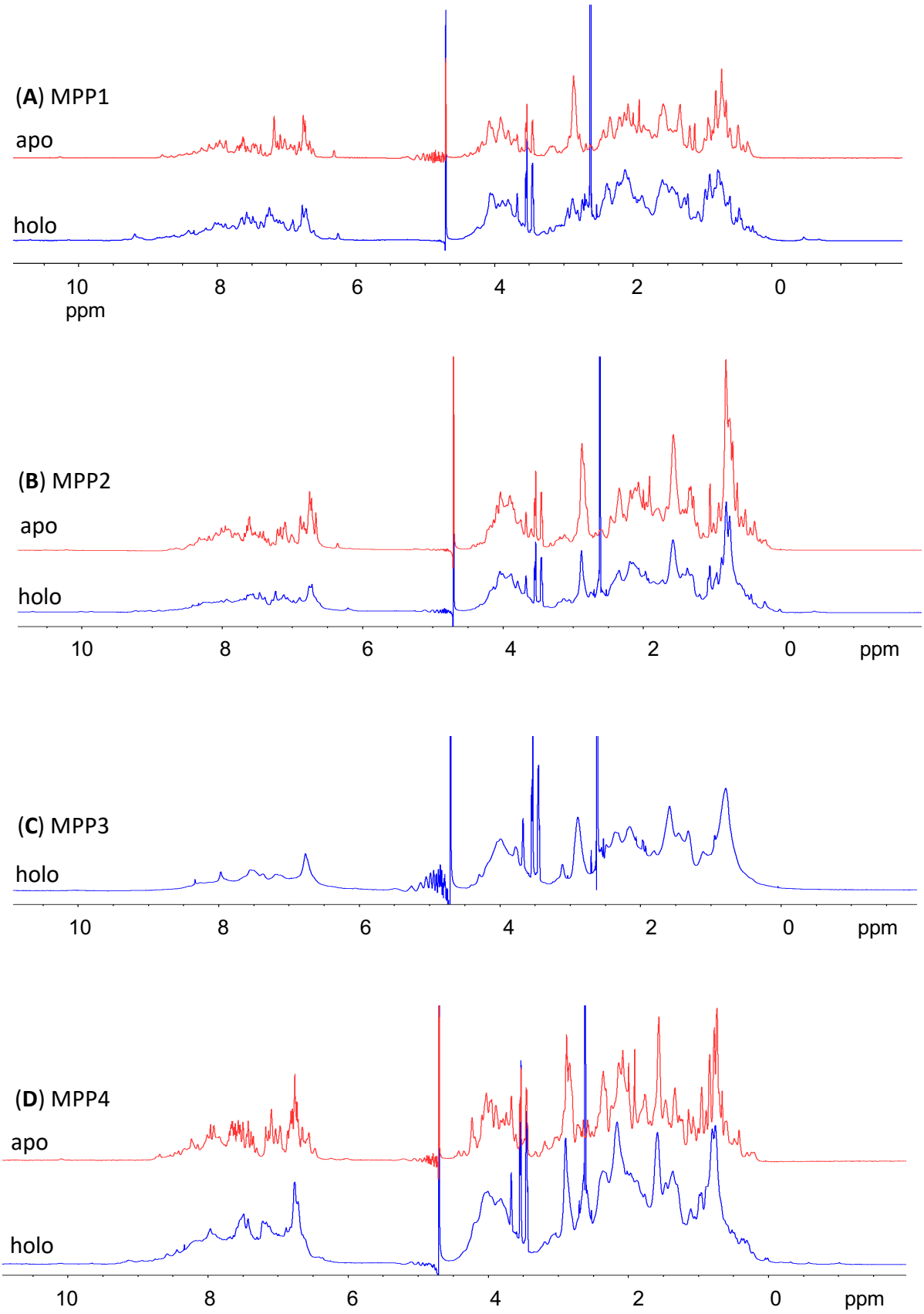
(A) MPP1
apo
holo
10
8
6
4
2
0
ppm
(B) MPP2
apo
holo
10
8
6
4
2
0
ppm
(C) MPP3
holo
10
8
6
4
2
0
ppm
(D) MPP4
apo
holo
10
8
6
4
2
0
ppm

Figure S5. 1D NMR comparison of MPP1-4. (**A**) for MPP1, amide chemical shift dispersion (6.3-8.8ppm) and upfield shifted methyl chemical shifts (<0.5ppm) indicated that the apo form is already well-structured. Upon ligand binding, the amide chemical shift dispersion is further expanded, and methyl chemical shifts are more upfield shifted. The same holds true for MPP2 (**B**). For MPP3 (**C**), the holo wasn't folded well based on the broad peak linewidth which indicates its molten globule state. For MPP4 (**D**), the apo is well structured but the holo is in a molten globule state.

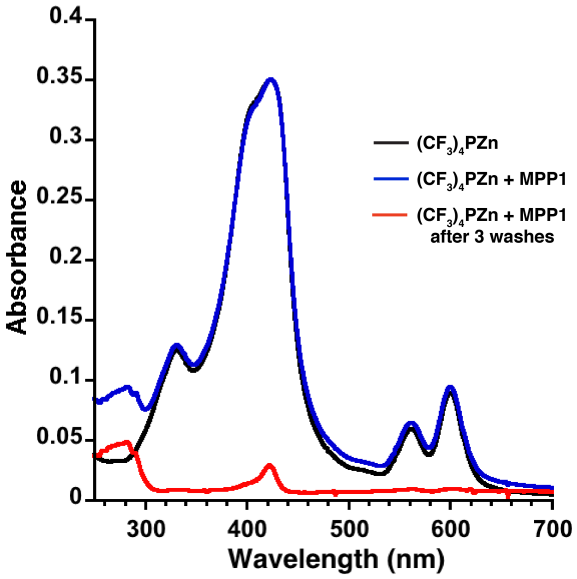

Figure S6. Electronic absorption spectra showing that $(CF_3)_4PZn$ does not bind to MPP1. Buffer conditions: 50 mM MES 150 mM NaCl pH 7.5.

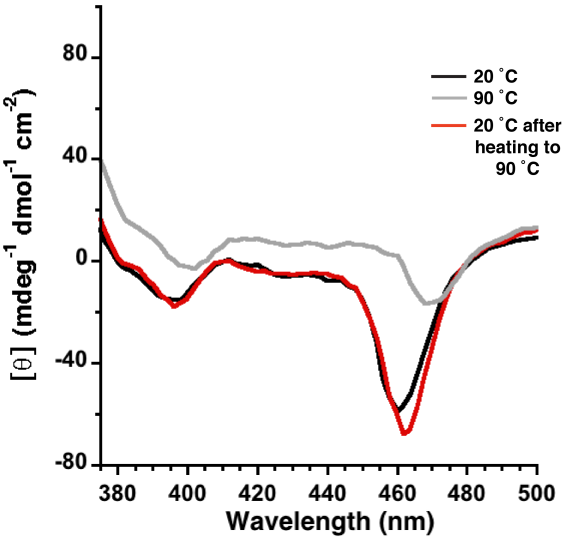

Figure S7. CD spectra showing that holo-MPP1 maintains its structure and MnDPP binding site after heating to 90 ˚C.

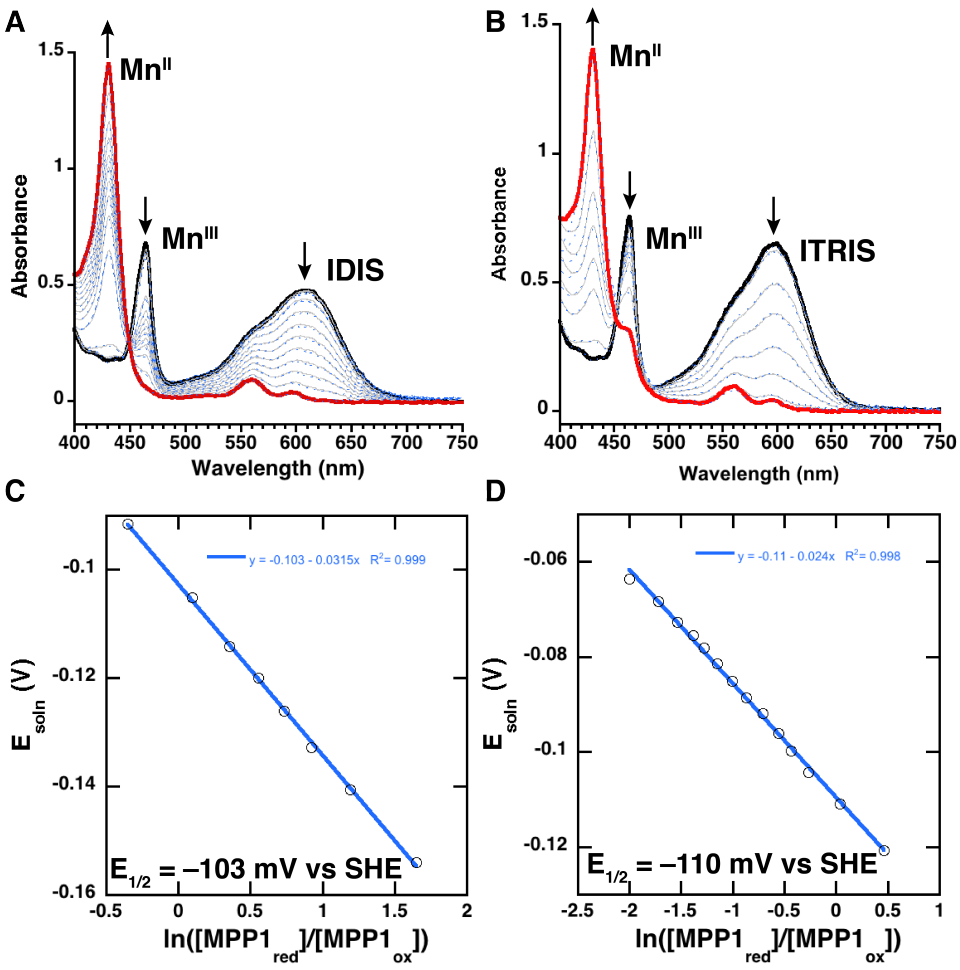

Figure S8. Equilibrium redox titration experiment. (**A**) and (**B**) show the electronic absorption spectra monitoring the reduction of Mn(III)MPP1 in the presence of IDIS and ITRIS, respectively. Blue dashed line is the fit of the data. (**C**) and (**D**) show the plotted solution potentials computed from the titration data for IDRIS and ITRIS, respectively, used to estimate the equilibrium midpoint potential of holoMPP1. Both plots have slopes that are consistent with a 1 e- Nernstian process.

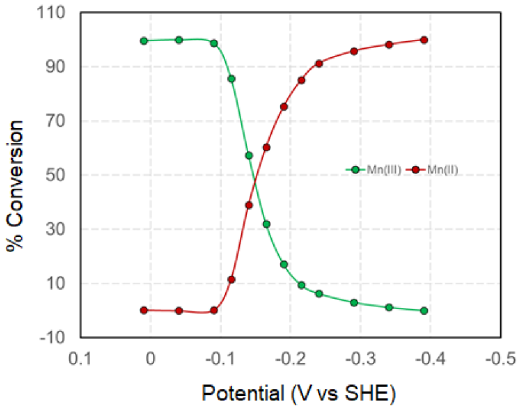

Figure S9. (A) Representative plot showing percent conversion from Mn(III)MPP1 to Mn(II)MPP1 during spectroelectrochemical measurements at pH 8 from 10 to -390 mV vs SHE. Mn(III)-MPP1 to Mn(II)-MPP1 conversion was based on their absorbances at 463 nm and 430 nm, respectively.

Table S2. Midpoint potentials from pH 6-8 measured by spectroelectrochemical titrations.

pH	$E_{1/2}(Mn^{II/III})$ (V vs SHE)
6	-0.11
7	-0.145
7.5	-0.146
8	-0.15

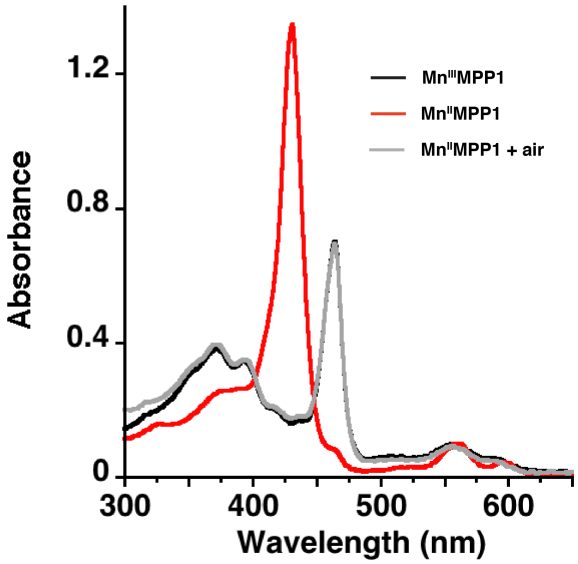

Figure S10. Absorption spectra of a degassed solution of Mn(III)MPP1 (black), after reduction with 1 equivalent of dithionite (red), and subsequent exposure to air (grey) showing the full recovery of the Mn(III) species.

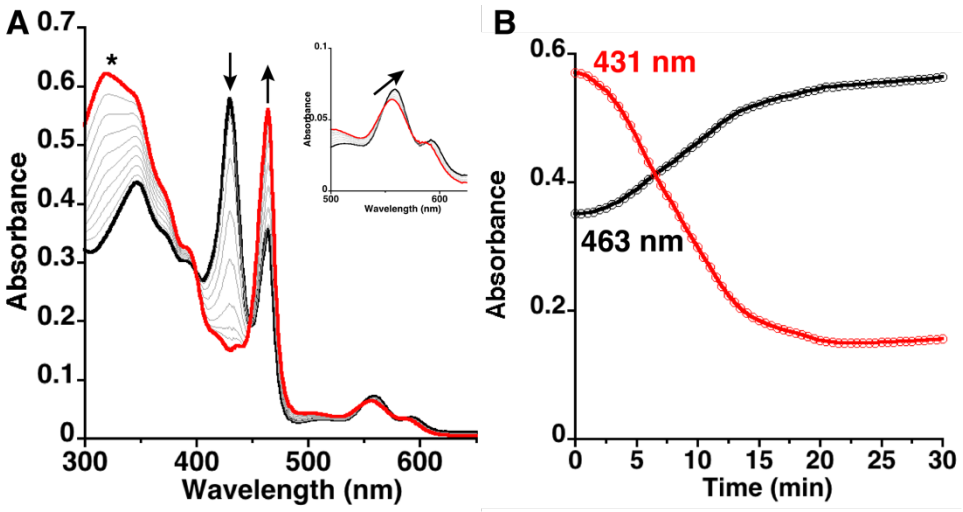

Figure S11. (**A**) Electronic absorption spectra showing the conversion of the Mn(V)-oxido species (black) back to the Mn(III)MPP1 species (red) with 30 s scans. Inset: Zoom in of changes in Q-bands. (**B**) Time trace of the reaction in (**A**). (*) indicates the absorbance from $NaIO_4$ reduction.

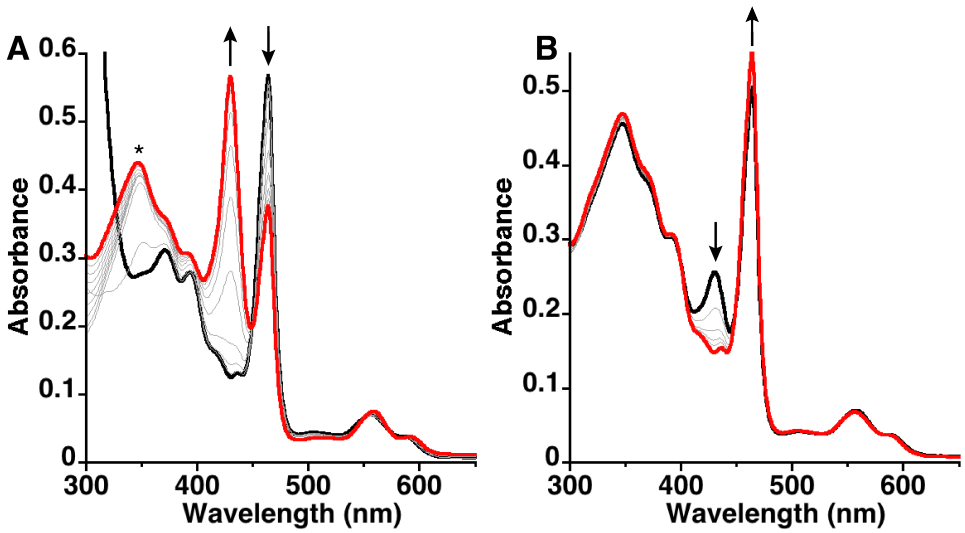

Figure S12. (**A**) Electronic absorption spectra showing the conversion of Mn(III)MPP1 (black) to the Mn(V)-oxido species (red) showing scans every 2-min. (**B**) Conversion of the Mn(V)-oxido species (black) to Mn(III)MPP1 (red) after addition of 10 equivalents of thioanisole. All reactions were performed in 50 mM sodium phosphate 150 mM NaCl pH 7.5.

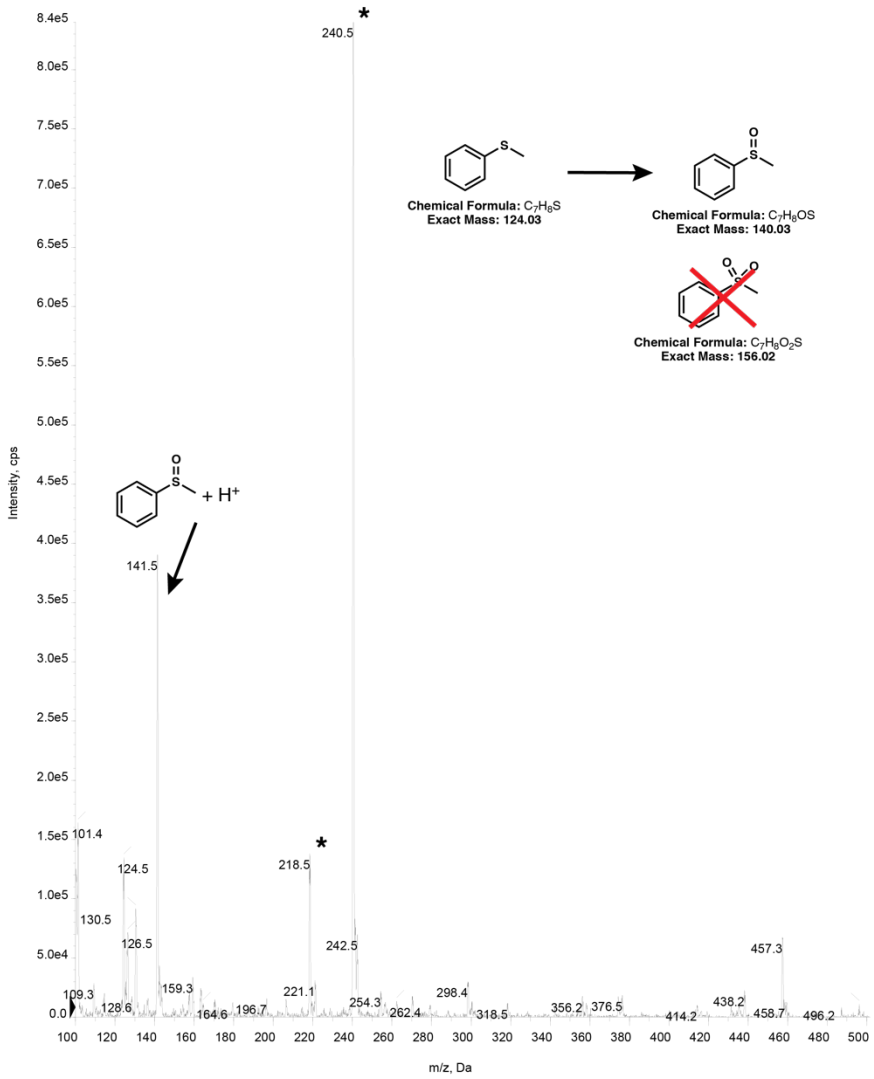

Figure S13. Mass spectrum of reaction mixture after addition of thioanisole to Mn(V)-oxido MPP1 showing formation of phenyl methyl sulfoxide and no evidence of phenyl methyl sulfone. (*) indicates masses from MES buffer.

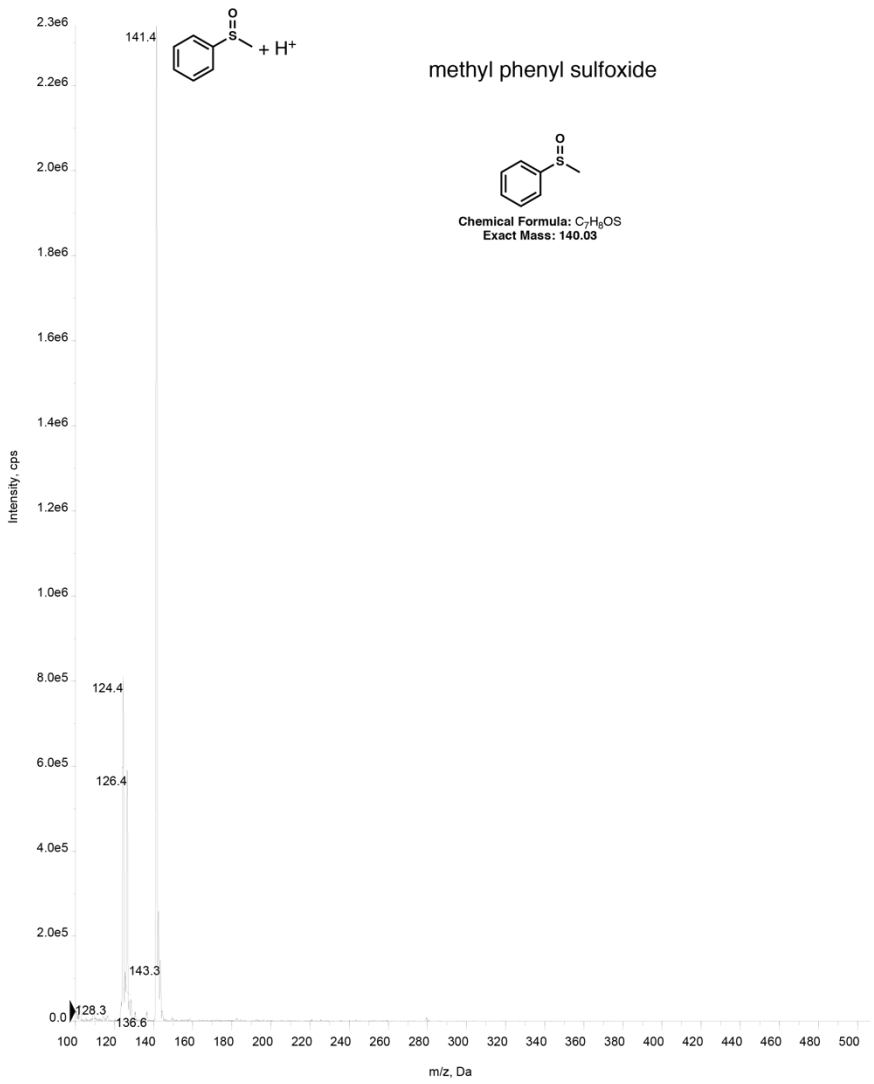

Figure S14. Mass spectrum of phenyl methyl sulfoxide standard.

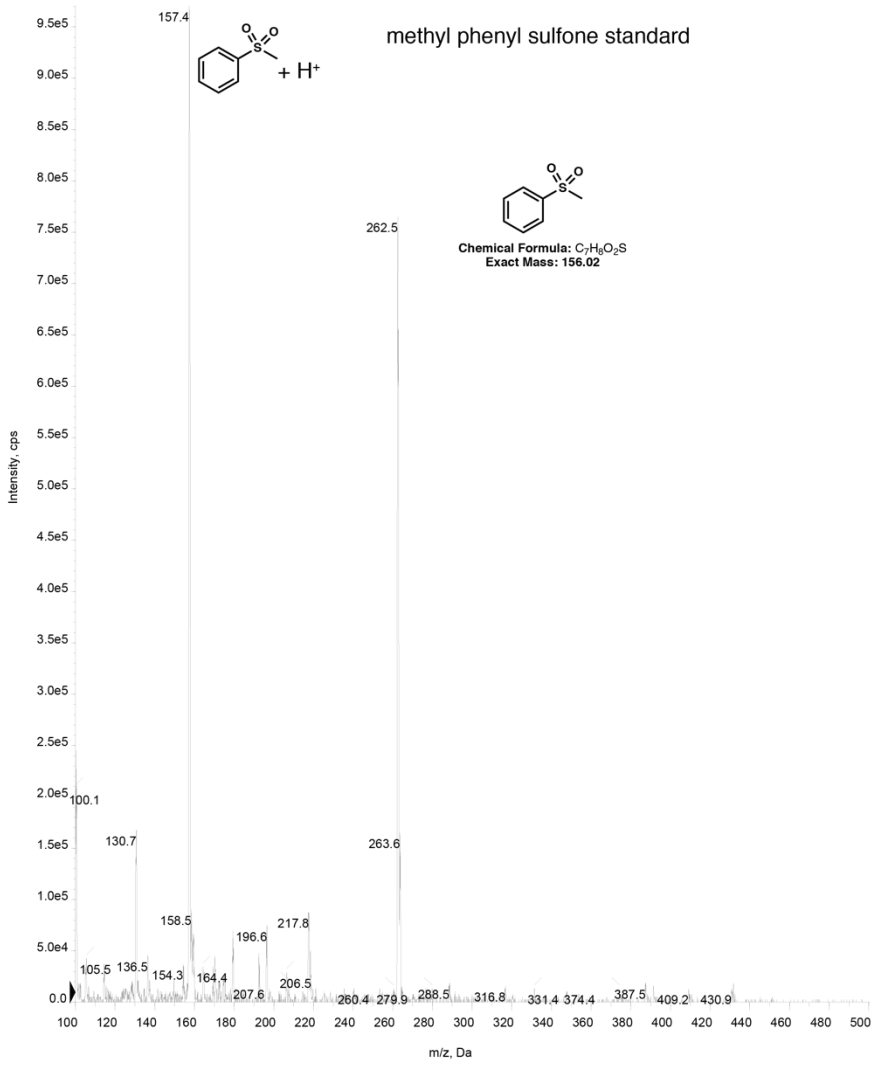

Figure S15. Mass spectrum of phenyl methyl sulfone standard.

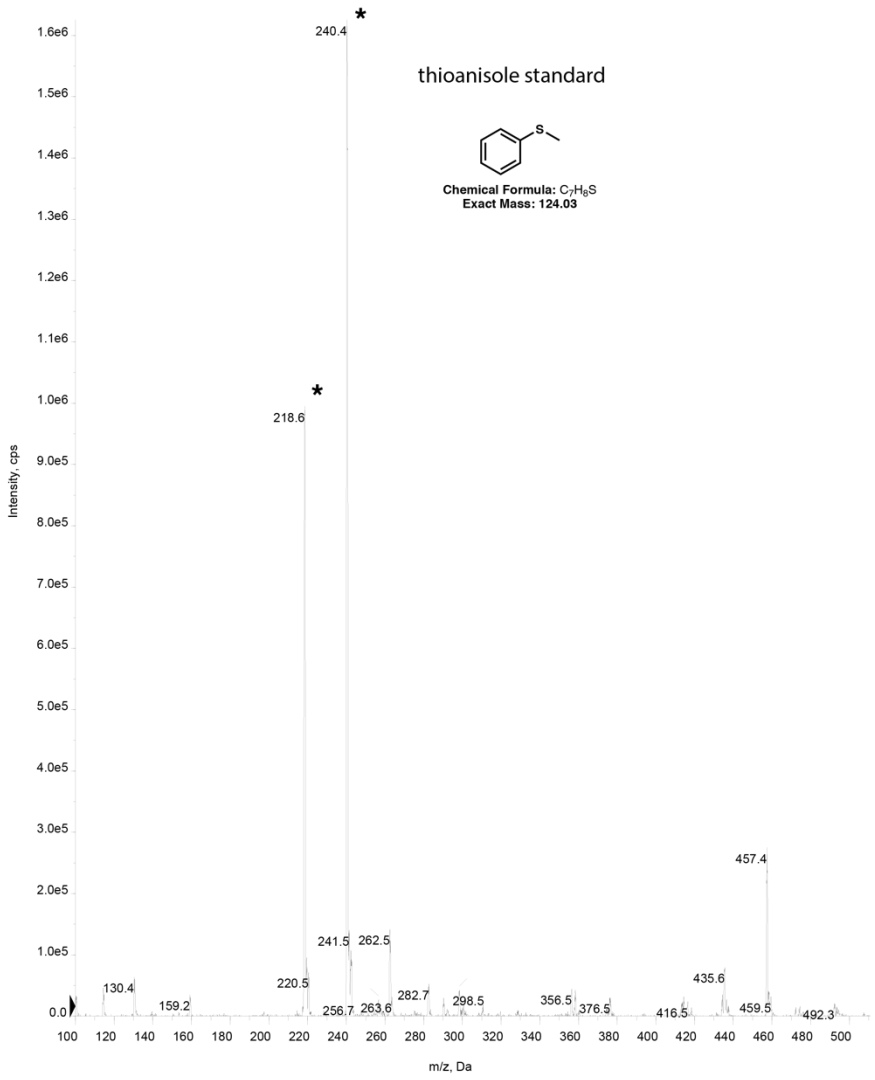

Figure S16. Mass spectrum of thioanisole standard. No signal corresponding to the thioanisole was observed. (*) indicated masses from MES buffer.

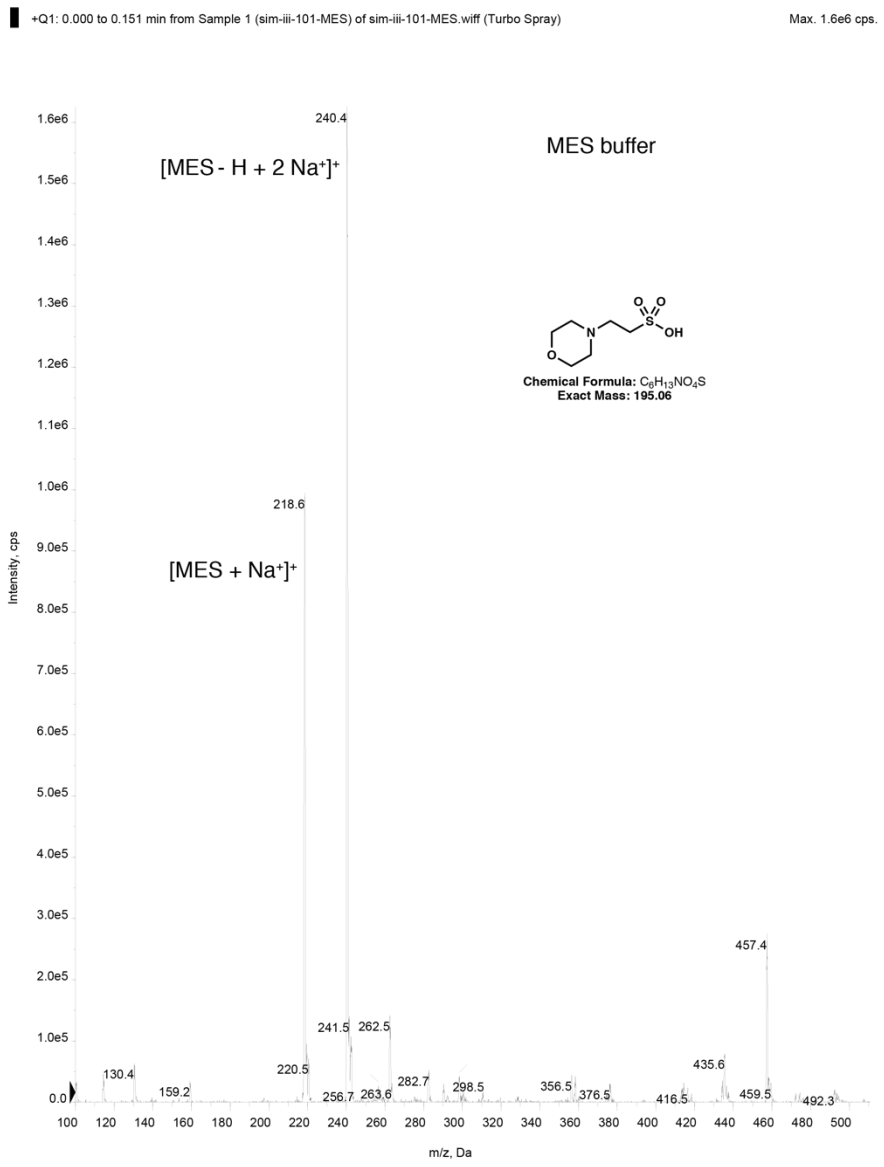

Figure S17. Mass spectrum of MES buffer solution.

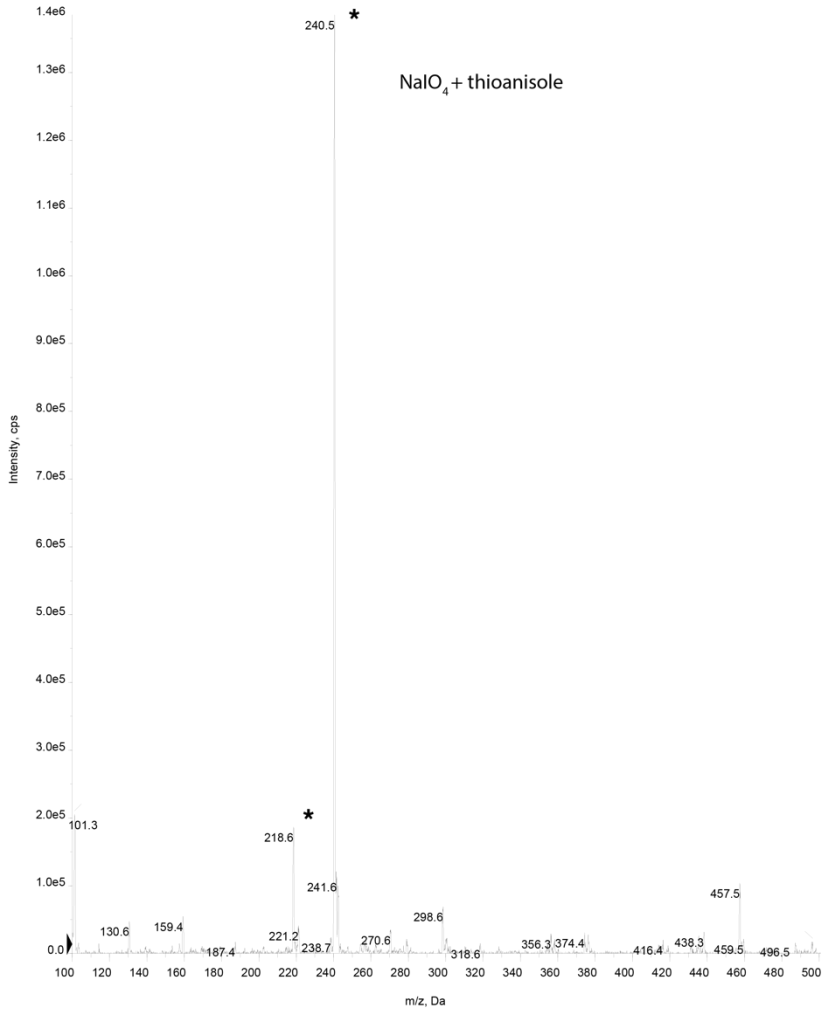

Figure S18. Mass spectrum of reaction mixture after incubating thioanisole and $NaIO_4$ in MES buffer. (*) indicates masses from MES buffer.

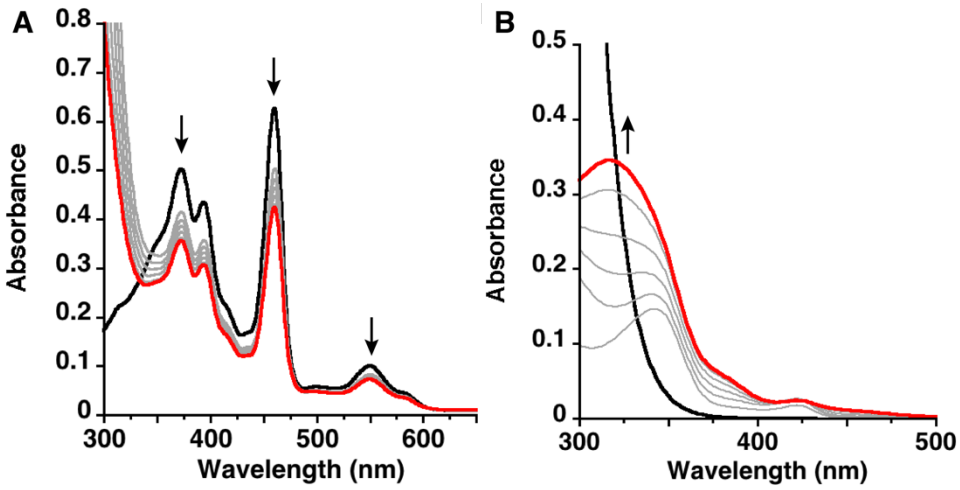

Figure S19. Electronic absorption spectra of reaction of Mn(III)DPP with $NaIO_4$ in buffer (**A**) and hydrolysis of $NaIO_4$ in buffer (**B**). Scan rates for (**A**) are 10 min. and (**B**) are 5 min.

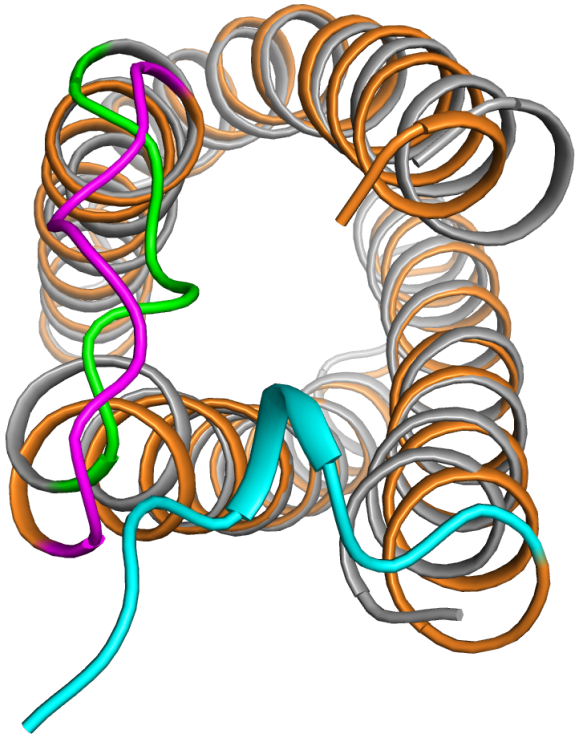

Figure S20. Cartoon representation of crystal structure of MPP1 (orange) aligned with the final Rosetta model of holo-MPP1 (grey) showing the displacement of loop BC (purple for structure, green for Rosetta model) by the His tag and TEV cleavage site (cyan).

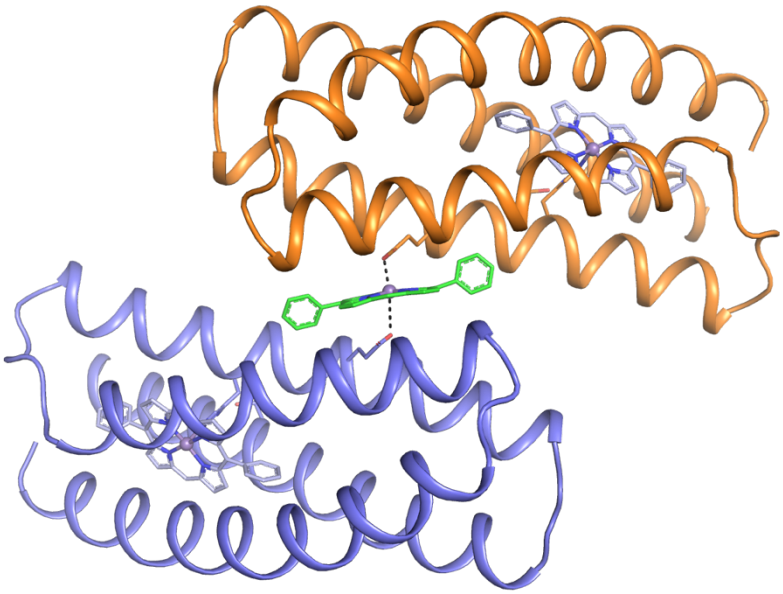

Figure S21. The crystal structure of holoMPP1 showing the symmetry related bundle (blue) and the secondary MnDPP (green) bound to the surface of the protein at a symmetry interface. Glu58 from symmetry-related subunits serve as axial ligands. Together, the Mn and non-functionalized miso-carbons lie along a C2 axis of the crystal. The inter-subunit MnDPP refines to 0.5 occupancy, as expected for a molecule that is shared between two crystallographically identical subunits. The protein was crystallized with a 1.2-fold excess of the porphyrin, which likely explains the interfacial porphyrin. If 40% of the protein-porphyrin complex (in a 1:1 ratio) crysatllized together with the 0.2-fold excess of porphyrin from the mother liquor this would account for the observed 1.5-fold excess in the crystal.

Table S3. Crystallographic data processing and refinement statistics.

Design Name	MPP1
Cofactor	Mn(III)DPP
PDB Code	7JRQ
Ligand 3-letter code	SM0
Data Processing	
Unit Cell	a,b,c = 45.322 Å, 45.322 Å, 164.22 Å; $\alpha,\beta,\gamma = 90$
Space Group	$P4_12_12$
Resolution (Å)	39.68 – 1.75
Highest Resolution Shell (Å)	1.75 – 1.80
No. of Unique Reflection	18042 (1510)
Multiplicity	8.7 (3.5)
I/sig(I)	5.2 (3.1)
R_{merge}	0.089 (2.4)
Completeness	99.4 (95.5)
CC(1/2)	0.977 (0.483)
SSRL BL	12-2
Structure Refinement	
R_{work}	0.195
R_{free}	0.2295
RMSD Bond Length (Å)	0.008
RMSD Bond Angle (˚)	0.7

Command lines, RosettaScript, and flags for flexible backbone sequence design protocol.

RosettaScript (rosettascript.xml).

```
<ROSETTASCRIPTS>
        <SCOREFXNS>
                <ScoreFunction name="cstscore" weights="ref2015">
                        <Reweight scoretype="aa_composition" weight="1.0"/>
                        <Reweight scoretype="atom_pair_constraint" weight="1"/>
                        <Reweight scoretype="angle_constraint" weight="1"/>
                        <Reweight scoretype="dihedral_constraint" weight="1"/>
                </ScoreFunction>
                <ScoreFunction name="cstscore_soft" weights="ref2015">
                        <Reweight scoretype="aa_composition" weight="1.0"/>
                        <Reweight scoretype="atom_pair_constraint" weight="1"/>
                        <Reweight scoretype="angle_constraint" weight="1"/>
                        <Reweight scoretype="dihedral_constraint" weight="1"/>
```

```
                <Reweight scoretype="fa_rep" weight="0.2"/>
            </ScoreFunction>
            <ScoreFunction name="score" weights="ref2015"/>
        </SCOREFXNS>
        <TASKOPERATIONS>
            <ReadResfile name="rr_ex" filename="resfile_ex1.txt"/>
            <ReadResfile name="rr_aro" filename="resfile_aro.txt"/>
            <ReadResfile name="rr_ex_3" filename="resfile_ex3.txt"/>
            <InitializeFromCommandline name="ifcl" />
        </TASKOPERATIONS>
        <FILTERS>
            <PackStat name="pstat_mc" threshold="0.48" repeats="10"/>
            <PackStat name="pstat_stop" threshold="0.65" repeats="10"/>
            <PackStat name="pstat" repeats="10" confidence="0"/>
        </FILTERS>
        <MOVERS>
            <ConstraintSetMover name="csts" add_constraints="1" cst_file="constraints.cst"/>
            <PackRotamersMover name="fixbb_aro" scorefxn="cstscore_soft"
task_operations="rr_aro,ifcl"/>
            <PackRotamersMover name="fixbb_ex_1" scorefxn="cstscore" task_operations="rr_ex,ifcl"/>
            <PackRotamersMover name="fixbb_ex_3" scorefxn="cstscore" task_operations="rr_ex_3,ifcl"/>
            <MinMover name="min_bb" scorefxn="cstscore" tolerance="0.000001" max_iter="10000"
chi="0" bb="1"/>
            <MinMover name="min_sc" scorefxn="cstscore" tolerance="0.000001" max_iter="10000"
chi="1" bb="0"/>
            <FastRelax name="fr" scorefxn="cstscore" relaxscript="rosettacon2018" />
            <ParsedProtocol name="custom_flex">
                <Add mover_name="fixbb_ex_1"/>
                <Add mover_name="fr"/>
            </ParsedProtocol>
            <ParsedProtocol name="final_flex">
                <Add mover_name="fixbb_ex_3"/>
                <Add mover_name="fr"/>
            </ParsedProtocol>
            <GenericMonteCarlo name="iterate" mover_name="custom_flex"
                                                filter_name="pstat_mc" trials="3" preapply="0"
                                                temperature="0" sample_type="high"
stopping_condition="pstat_stop"
                                                saved_accept_file_name="last_accepted.pdb"
recover_low="1"/>
            <GenericMonteCarlo name="final" mover_name="final_flex"
                                                filter_name="pstat_mc" trials="1" preapply="0"
                                                temperature ="0" sample_type="high"
                                                saved_accept_file_name="last_accepted.pdb"
recover_low="1"/>
        </MOVERS>
        <APPLY_TO_POSE>
        </APPLY_TO_POSE>
        <PROTOCOLS>
            <Add mover_name="csts"/>
            <Add mover_name="fixbb_aro"/>
            <Add mover_name="min_sc"/>
            <Add mover_name="min_bb"/>
            <Add mover_name="iterate"/>
            <Add mover_name="final"/>
            <Add filter_name="pstat"/>
```

```
        </PROTOCOLS>
        <OUTPUT scorefxn="cstscore"/>
</ROSETTASCRIPTS>
```

Contents of Constraint File (constraints.cst).

```
#His MnDPP Bond
AtomPair NE2 50A MN1 1X HARMONIC 2.1 0.1
Angle MN1 1X NE2 50A ND1 50A CIRCULARHARMONIC 2.687 .2
Angle MN1 1X NE2 50A CG 50A CIRCULARHARMONIC 2.426 .2

#Thr His Hbond
AtomPair ND1 50A OG1 13A HARMONIC 2.8 0.1
Angle OG1 13A ND1 50A CE1 50A CIRCULARHARMONIC 2.370 .2
Angle OG1 13A ND1 50A CG 50A CIRCULARHARMONIC 2.007 .2
```

Flags (options.txt).

```
-nstruct 100
-out:path:pdb output
-out:path:score output
-extra_res_fa MDP.params
-s input_model.pdb
```

Command line inputs.

~/rosetta_bin_linux_2018.33.60351_bundle/main/source/bin/rosetta_scripts.static.linuxgccrelease -database ~/rosetta_bin_linux_2018.33.60351_bundle/main/database/ -parser:protocol RosettaScript.xml @options.txt

Contents of residue file (resfile_aro.txt).

```
NATRO
ALLAAxc
NOTAA MCT
USE_INPUT_SC
start

1 A PIKAA ASTG EX ARO 1 LEVEL 3 EX ARO 2 LEVEL 3
2 A ALLAAxc NOTAA MC EX ARO 1 LEVEL 3 EX ARO 2 LEVEL 3
3 A ALLAAxc NOTAA MC EX ARO 1 LEVEL 3 EX ARO 2 LEVEL 3
4 A ALLAAxc NOTAA MC EX ARO 1 LEVEL 3 EX ARO 2 LEVEL 3
5 A ALLAAxc NOTAA MC EX ARO 1 LEVEL 3 EX ARO 2 LEVEL 3
6 A APOLAR NOTAA MCT EX ARO 1 LEVEL 3 EX ARO 2 LEVEL 3
7 A APOLAR NOTAA MCT EX ARO 1 LEVEL 3 EX ARO 2 LEVEL 3
11 A ALLAAxc NOTAA MC EX ARO 1 LEVEL 3 EX ARO 2 LEVEL 3
13 A PIKAA T
14 A APOLAR PIKAA A EX ARO 1 LEVEL 3 EX ARO 2 LEVEL 3
17 A APOLAR NOTAA MCT EX ARO 1 LEVEL 3 EX ARO 2 LEVEL 3
18 A APOLAR PIKAA ATV EX ARO 1 LEVEL 3 EX ARO 2 LEVEL 3
20 A APOLAR NOTAA MCT EX ARO 1 LEVEL 3 EX ARO 2 LEVEL 3
21 A APOLAR NOTAA MCT EX ARO 1 LEVEL 3 EX ARO 2 LEVEL 3
24 A APOLAR NOTAA MCT EX ARO 1 LEVEL 3 EX ARO 2 LEVEL 3
27 A APOLAR NOTAA MCT EX ARO 1 LEVEL 3 EX ARO 2 LEVEL 3
28 A APOLAR NOTAA MCT EX ARO 1 LEVEL 3 EX ARO 2 LEVEL 3
```

31 A PIKAA G EX ARO 1 LEVEL 3 EX ARO 2 LEVEL 3
32 A PIKAA D EX ARO 1 LEVEL 3 EX ARO 2 LEVEL 3

36 A APOLAR NOTAA MCT EX ARO 1 LEVEL 3 EX ARO 2 LEVEL 3
39 A APOLAR NOTAA MCT EX ARO 1 LEVEL 3 EX ARO 2 LEVEL 3
40 A APOLAR NOTAA MCT EX ARO 1 LEVEL 3 EX ARO 2 LEVEL 3
43 A APOLAR NOTAA MCT EX ARO 1 LEVEL 3 EX ARO 2 LEVEL 3
46 A APOLAR NOTAA MCT EX ARO 1 LEVEL 3 EX ARO 2 LEVEL 3
47 A APOLAR NOTAA MCT EX ARO 1 LEVEL 3 EX ARO 2 LEVEL 3
50 A PIKAA H
53 A APOLAR NOTAA MCT EX ARO 1 LEVEL 3 EX ARO 2 LEVEL 3
54 A APOLAR NOTAA MCT EX ARO 1 LEVEL 3 EX ARO 2 LEVEL 3
55 A PIKAA ED EX ARO 1 LEVEL 3 EX ARO 2 LEVEL 3
56 A PIKAA QN EX ARO 1 LEVEL 3 EX ARO 2 LEVEL 3

57 A PIKAA G EX ARO 1 LEVEL 3 EX ARO 2 LEVEL 3

58 A ALLAAxc NOTAA M EX ARO 1 LEVEL 3 EX ARO 2 LEVEL 3
59 A ALLAAxc NOTAA M EX ARO 1 LEVEL 3 EX ARO 2 LEVEL 3
60 A ALLAAxc NOTAA M EX ARO 1 LEVEL 3 EX ARO 2 LEVEL 3
61 A PIKAA G NOTAA M EX ARO 1 LEVEL 3 EX ARO 2 LEVEL 3
62 A ALLAAxc NOTAA MWFY EX ARO 1 LEVEL 3 EX ARO 2 LEVEL 3
63 A PIKAA LIVA EX ARO 1 LEVEL 3 EX ARO 2 LEVEL 3
64 A PIKAA STP EX ARO 1 LEVEL 3 EX ARO 2 LEVEL 3

65 A PIKAA AST EX ARO 1 LEVEL 3 EX ARO 2 LEVEL 3
66 A PIKAA ED EX ARO 1 LEVEL 3 EX ARO 2 LEVEL 3
67 A APOLAR NOTAA MCT EX ARO 1 LEVEL 3 EX ARO 2 LEVEL 3
68 A PIKAA A EX ARO 1 LEVEL 3 EX ARO 2 LEVEL 3
69 A PIKAA K EX ARO 1 LEVEL 3 EX ARO 2 LEVEL 3
70 A PIKAA QN EX ARO 1 LEVEL 3 EX ARO 2 LEVEL 3
71 A PIKAA G EX ARO 1 LEVEL 3 EX ARO 2 LEVEL 3
74 A APOLAR NOTAA MCT EX ARO 1 LEVEL 3 EX ARO 2 LEVEL 3
78 A APOLAR NOTAA MCT EX ARO 1 LEVEL 3 EX ARO 2 LEVEL 3
81 A APOLAR NOTAA MCT EX ARO 1 LEVEL 3 EX ARO 2 LEVEL 3
84 A APOLAR NOTAA MCT EX ARO 1 LEVEL 3 EX ARO 2 LEVEL 3
85 A APOLAR NOTAA MCT EX ARO 1 LEVEL 3 EX ARO 2 LEVEL 3

88 A PIKAA G EX ARO 1 LEVEL 3 EX ARO 2 LEVEL 3
89 A PIKAA D EX ARO 1 LEVEL 3 EX ARO 2 LEVEL 3

93 A APOLAR NOTAA MCT EX ARO 1 LEVEL 3 EX ARO 2 LEVEL 3
96 A APOLAR NOTAA MCT EX ARO 1 LEVEL 3 EX ARO 2 LEVEL 3
97 A APOLAR NOTAA MCT EX ARO 1 LEVEL 3 EX ARO 2 LEVEL 3
100 A APOLAR NOTAA MCT EX ARO 1 LEVEL 3 EX ARO 2 LEVEL 3
103 A APOLAR NOTAA MCT EX ARO 1 LEVEL 3 EX ARO 2 LEVEL 3
104 A APOLAR NOTAA MCT EX ARO 1 LEVEL 3 EX ARO 2 LEVEL 3
107 A APOLAR NOTAA MCT EX ARO 1 LEVEL 3 EX ARO 2 LEVEL 3
108 A PIKAA VLT EX ARO 1 LEVEL 3 EX ARO 2 LEVEL 3
111 A PIKAA G EX ARO 1 LEVEL 3 EX ARO 2 LEVEL 3
112 A APOLAR NOTAA MC EX ARO 1 LEVEL 3 EX ARO 2 LEVEL 3
113 A ALLAAxc NOTAA MCH EX ARO 1 LEVEL 3 EX ARO 2 LEVEL 3
114 A APOLAR NOTAA MCW EX ARO 1 LEVEL 3 EX ARO 2 LEVEL 3
115 A APOLAR NOTAA MC EX ARO 1 LEVEL 3 EX ARO 2 LEVEL 3
116 A ALLAAxc NOTAA MCH EX ARO 1 LEVEL 3 EX ARO 2 LEVEL 3

117 A ALLAAxc NOTAA MCH EX ARO 1 LEVEL 3 EX ARO 2 LEVEL 3
118 A POLAR NOTAA MCH EX ARO 1 LEVEL 3 EX ARO 2 LEVEL 3

Contents of residue file (resfile_ex1.txt).

NATRO
ALLAAxc
NOTAA MCT
USE_INPUT_SC
start

1 A PIKAA ASTG EX 1 LEVEL 1 EX 2 LEVEL 1
2 A ALLAAxc NOTAA MC EX 1 LEVEL 1 EX 2 LEVEL 1
3 A ALLAAxc NOTAA MC EX 1 LEVEL 1 EX 2 LEVEL 1
4 A ALLAAxc NOTAA MC EX 1 LEVEL 1 EX 2 LEVEL 1
5 A ALLAAxc NOTAA MC EX 1 LEVEL 1 EX 2 LEVEL 1
6 A APOLAR NOTAA MCT EX 1 LEVEL 1 EX 2 LEVEL 1
7 A APOLAR NOTAA MCT EX 1 LEVEL 1 EX 2 LEVEL 1
11 A ALLAAxc NOTAA MC EX 1 LEVEL 1 EX 2 LEVEL 1
13 A PIKAA T
14 A APOLAR PIKAA A EX 1 LEVEL 1 EX 2 LEVEL 1
17 A APOLAR NOTAA MCT EX 1 LEVEL 1 EX 2 LEVEL 1
18 A APOLAR PIKAA ATV EX 1 LEVEL 1 EX 2 LEVEL 1
20 A APOLAR NOTAA MCT EX 1 LEVEL 1 EX 2 LEVEL 1
21 A APOLAR NOTAA MCT EX 1 LEVEL 1 EX 2 LEVEL 1
24 A APOLAR NOTAA MCT EX 1 LEVEL 1 EX 2 LEVEL 1
27 A APOLAR NOTAA MCT EX 1 LEVEL 1 EX 2 LEVEL 1
28 A APOLAR NOTAA MCT EX 1 LEVEL 1 EX 2 LEVEL 1

31 A PIKAA G EX 1 LEVEL 1 EX 2 LEVEL 1
32 A PIKAA D EX 1 LEVEL 1 EX 2 LEVEL 1

36 A APOLAR NOTAA MCT EX 1 LEVEL 1 EX 2 LEVEL 1
39 A APOLAR NOTAA MCT EX 1 LEVEL 1 EX 2 LEVEL 1
40 A APOLAR NOTAA MCT EX 1 LEVEL 1 EX 2 LEVEL 1
43 A APOLAR NOTAA MCT EX 1 LEVEL 1 EX 2 LEVEL 1
46 A APOLAR NOTAA MCT EX 1 LEVEL 1 EX 2 LEVEL 1
47 A APOLAR NOTAA MCT EX 1 LEVEL 1 EX 2 LEVEL 1
50 A PIKAA H
53 A APOLAR NOTAA MCT EX 1 LEVEL 1 EX 2 LEVEL 1
54 A APOLAR NOTAA MCT EX 1 LEVEL 1 EX 2 LEVEL 1
55 A PIKAA ED EX 1 LEVEL 1 EX 2 LEVEL 1
56 A PIKAA QN EX 1 LEVEL 1 EX 2 LEVEL 1

57 A PIKAA G EX 1 LEVEL 1 EX 2 LEVEL 1

58 A ALLAAxc NOTAA M EX 1 LEVEL 1 EX 2 LEVEL 1
59 A ALLAAxc NOTAA M EX 1 LEVEL 1 EX 2 LEVEL 1
60 A ALLAAxc NOTAA M EX 1 LEVEL 1 EX 2 LEVEL 1
61 A PIKAA G NOTAA M EX 1 LEVEL 1 EX 2 LEVEL 1
62 A ALLAAxc NOTAA MWFY EX 1 LEVEL 1 EX 2 LEVEL 1
63 A PIKAA LIVA EX 1 LEVEL 1 EX 2 LEVEL 1
64 A PIKAA STP EX 1 LEVEL 1 EX 2 LEVEL 1

65 A PIKAA AST EX 1 LEVEL 1 EX 2 LEVEL 1
66 A PIKAA ED EX 1 LEVEL 1 EX 2 LEVEL 1
67 A APOLAR NOTAA MCT EX 1 LEVEL 1 EX 2 LEVEL 1

68 A PIKAA A EX 1 LEVEL 1 EX 2 LEVEL 1
69 A PIKAA K EX 1 LEVEL 1 EX 2 LEVEL 1
70 A PIKAA QN EX 1 LEVEL 1 EX 2 LEVEL 1
71 A PIKAA G EX 1 LEVEL 1 EX 2 LEVEL 1
74 A APOLAR NOTAA MCT EX 1 LEVEL 1 EX 2 LEVEL 1
78 A APOLAR NOTAA MCT EX 1 LEVEL 1 EX 2 LEVEL 1
81 A APOLAR NOTAA MCT EX 1 LEVEL 1 EX 2 LEVEL 1
84 A APOLAR NOTAA MCT EX 1 LEVEL 1 EX 2 LEVEL 1
85 A APOLAR NOTAA MCT EX 1 LEVEL 1 EX 2 LEVEL 1

88 A PIKAA G EX 1 LEVEL 1 EX 2 LEVEL 1
89 A PIKAA D EX 1 LEVEL 1 EX 2 LEVEL 1

93 A APOLAR NOTAA MCT EX 1 LEVEL 1 EX 2 LEVEL 1
96 A APOLAR NOTAA MCT EX 1 LEVEL 1 EX 2 LEVEL 1
97 A APOLAR NOTAA MCT EX 1 LEVEL 1 EX 2 LEVEL 1
100 A APOLAR NOTAA MCT EX 1 LEVEL 1 EX 2 LEVEL 1
103 A APOLAR NOTAA MCT EX 1 LEVEL 1 EX 2 LEVEL 1
104 A APOLAR NOTAA MCT EX 1 LEVEL 1 EX 2 LEVEL 1
107 A APOLAR NOTAA MCT EX 1 LEVEL 1 EX 2 LEVEL 1
108 A PIKAA VLT EX 1 LEVEL 1 EX 2 LEVEL 1
111 A PIKAA G EX 1 LEVEL 1 EX 2 LEVEL 1
112 A APOLAR NOTAA MC EX 1 LEVEL 1 EX 2 LEVEL 1
113 A ALLAAxc NOTAA MCH EX 1 LEVEL 1 EX 2 LEVEL 1
114 A APOLAR NOTAA MCW EX 1 LEVEL 1 EX 2 LEVEL 1
115 A APOLAR NOTAA MC EX 1 LEVEL 1 EX 2 LEVEL 1
116 A ALLAAxc NOTAA MCH EX 1 LEVEL 1 EX 2 LEVEL 1
117 A ALLAAxc NOTAA MCH EX 1 LEVEL 1 EX 2 LEVEL 1
118 A POLAR NOTAA MCH EX 1 LEVEL 1 EX 2 LEVEL 1

Contents of residue file (resfile_ex3.txt).

NATRO
ALLAAxc
NOTAA MCT
USE_INPUT_SC
start

1 A PIKAA ASTG EX 1 LEVEL 3 EX 2 LEVEL 3
2 A ALLAAxc NOTAA MC EX 1 LEVEL 3 EX 2 LEVEL 3
3 A ALLAAxc NOTAA MC EX 1 LEVEL 3 EX 2 LEVEL 3
4 A ALLAAxc NOTAA MC EX 1 LEVEL 3 EX 2 LEVEL 3
5 A ALLAAxc NOTAA MC EX 1 LEVEL 3 EX 2 LEVEL 3
6 A APOLAR NOTAA MCT EX 1 LEVEL 3 EX 2 LEVEL 3
7 A APOLAR NOTAA MCT EX 1 LEVEL 3 EX 2 LEVEL 3
11 A ALLAAxc NOTAA MC EX 1 LEVEL 3 EX 2 LEVEL 3
13 A PIKAA T
14 A APOLAR PIKAA A EX 1 LEVEL 3 EX 2 LEVEL 3
17 A APOLAR NOTAA MCT EX 1 LEVEL 3 EX 2 LEVEL 3
18 A APOLAR PIKAA ATV EX 1 LEVEL 3 EX 2 LEVEL 3
20 A APOLAR NOTAA MCT EX 1 LEVEL 3 EX 2 LEVEL 3
21 A APOLAR NOTAA MCT EX 1 LEVEL 3 EX 2 LEVEL 3
24 A APOLAR NOTAA MCT EX 1 LEVEL 3 EX 2 LEVEL 3
27 A APOLAR NOTAA MCT EX 1 LEVEL 3 EX 2 LEVEL 3
28 A APOLAR NOTAA MCT EX 1 LEVEL 3 EX 2 LEVEL 3

31 A PIKAA G EX 1 LEVEL 3 EX 2 LEVEL 3

32 A PIKAA D EX 1 LEVEL 3 EX 2 LEVEL 3

36 A APOLAR NOTAA MCT EX 1 LEVEL 3 EX 2 LEVEL 3
39 A APOLAR NOTAA MCT EX 1 LEVEL 3 EX 2 LEVEL 3
40 A APOLAR NOTAA MCT EX 1 LEVEL 3 EX 2 LEVEL 3
43 A APOLAR NOTAA MCT EX 1 LEVEL 3 EX 2 LEVEL 3
46 A APOLAR NOTAA MCT EX 1 LEVEL 3 EX 2 LEVEL 3
47 A APOLAR NOTAA MCT EX 1 LEVEL 3 EX 2 LEVEL 3
50 A PIKAA H
53 A APOLAR NOTAA MCT EX 1 LEVEL 3 EX 2 LEVEL 3
54 A APOLAR NOTAA MCT EX 1 LEVEL 3 EX 2 LEVEL 3
55 A PIKAA ED EX 1 LEVEL 3 EX 2 LEVEL 3
56 A PIKAA QN EX 1 LEVEL 3 EX 2 LEVEL 3

57 A PIKAA G EX 1 LEVEL 3 EX 2 LEVEL 3

58 A ALLAAxc NOTAA M EX 1 LEVEL 3 EX 2 LEVEL 3
59 A ALLAAxc NOTAA M EX 1 LEVEL 3 EX 2 LEVEL 3
60 A ALLAAxc NOTAA M EX 1 LEVEL 3 EX 2 LEVEL 3
61 A PIKAA G NOTAA M EX 1 LEVEL 3 EX 2 LEVEL 3
62 A ALLAAxc NOTAA MWFY EX 1 LEVEL 3 EX 2 LEVEL 3
63 A PIKAA LIVA EX 1 LEVEL 3 EX 2 LEVEL 3
64 A PIKAA STP EX 1 LEVEL 3 EX 2 LEVEL 3

65 A PIKAA AST EX 1 LEVEL 3 EX 2 LEVEL 3
66 A PIKAA ED EX 1 LEVEL 3 EX 2 LEVEL 3
67 A APOLAR NOTAA MCT EX 1 LEVEL 3 EX 2 LEVEL 3
68 A PIKAA A EX 1 LEVEL 3 EX 2 LEVEL 3
69 A PIKAA K EX 1 LEVEL 3 EX 2 LEVEL 3
70 A PIKAA QN EX 1 LEVEL 3 EX 2 LEVEL 3
71 A PIKAA G EX 1 LEVEL 3 EX 2 LEVEL 3
74 A APOLAR NOTAA MCT EX 1 LEVEL 3 EX 2 LEVEL 3
78 A APOLAR NOTAA MCT EX 1 LEVEL 3 EX 2 LEVEL 3
81 A APOLAR NOTAA MCT EX 1 LEVEL 3 EX 2 LEVEL 3
84 A APOLAR NOTAA MCT EX 1 LEVEL 3 EX 2 LEVEL 3
85 A APOLAR NOTAA MCT EX 1 LEVEL 3 EX 2 LEVEL 3

88 A PIKAA G EX 1 LEVEL 3 EX 2 LEVEL 3
89 A PIKAA D EX 1 LEVEL 3 EX 2 LEVEL 3

93 A APOLAR NOTAA MCT EX 1 LEVEL 3 EX 2 LEVEL 3
96 A APOLAR NOTAA MCT EX 1 LEVEL 3 EX 2 LEVEL 3
97 A APOLAR NOTAA MCT EX 1 LEVEL 3 EX 2 LEVEL 3
100 A APOLAR NOTAA MCT EX 1 LEVEL 3 EX 2 LEVEL 3
103 A APOLAR NOTAA MCT EX 1 LEVEL 3 EX 2 LEVEL 3
104 A APOLAR NOTAA MCT EX 1 LEVEL 3 EX 2 LEVEL 3
107 A APOLAR NOTAA MCT EX 1 LEVEL 3 EX 2 LEVEL 3
108 A PIKAA VLT EX 1 LEVEL 3 EX 2 LEVEL 3
111 A PIKAA G EX 1 LEVEL 3 EX 2 LEVEL 3
112 A APOLAR NOTAA MC EX 1 LEVEL 3 EX 2 LEVEL 3
113 A ALLAAxc NOTAA MCH EX 1 LEVEL 3 EX 2 LEVEL 3
114 A APOLAR NOTAA MCW EX 1 LEVEL 3 EX 2 LEVEL 3
115 A APOLAR NOTAA MC EX 1 LEVEL 3 EX 2 LEVEL 3
116 A ALLAAxc NOTAA MCH EX 1 LEVEL 3 EX 2 LEVEL 3
117 A ALLAAxc NOTAA MCH EX 1 LEVEL 3 EX 2 LEVEL 3
118 A POLAR NOTAA MCH EX 1 LEVEL 3 EX 2 LEVEL 3

Contents of MnDPP paramters file (MDP.params).

```
NAME MDP
IO_STRING MDP Z
TYPE LIGAND
AA UNK
ATOM MN1  Mn    X   2.03
ATOM  N1  Npro  X   -0.34
ATOM  C4  aroC  X   -0.09
ATOM  C3  aroC  X   -0.09
ATOM  C2  aroC  X   -0.09
ATOM  C1  aroC  X   -0.09
ATOM  C20 CH1   X   -0.06
ATOM  C19 aroC  X   -0.09
ATOM  N4  Npro  X   -0.34
ATOM  C16 aroC  X   -0.09
ATOM  C15 CH1   X   -0.06
ATOM  C14 aroC  X   -0.09
ATOM  N3  Npro  X   -0.34
ATOM  C11 aroC  X   -0.09
ATOM  C10 CH1   X   -0.06
ATOM  C9  aroC  X   -0.09
ATOM  N2  Npro  X   -0.34
ATOM  C6  aroC  X   -0.09
ATOM  C5  CH1   X   -0.06
ATOM  C21 aroC  X   -0.09
ATOM  C22 aroC  X   -0.09
ATOM  C23 aroC  X   -0.09
ATOM  C24 aroC  X   -0.09
ATOM  C25 aroC  X   -0.09
ATOM  C26 aroC  X   -0.09
ATOM  H13 Haro  X   0.14
ATOM  H12 Haro  X   0.14
ATOM  H11 Haro  X   0.14
ATOM  H10 Haro  X   0.14
ATOM  H9  Haro  X   0.14
ATOM  C7  aroC  X   -0.09
ATOM  C8  aroC  X   -0.09
ATOM  H4  Haro  X   0.14
ATOM  H3  Haro  X   0.14
ATOM  H21 Hapo  X   0.12
ATOM  C12 aroC  X   -0.09
ATOM  C13 aroC  X   -0.09
ATOM  H6  Haro  X   0.14
ATOM  H5  Haro  X   0.14
ATOM  C27 aroC  X   -0.09
ATOM  C28 aroC  X   -0.09
ATOM  C29 aroC  X   -0.09
ATOM  C30 aroC  X   -0.09
ATOM  C31 aroC  X   -0.09
ATOM  C32 aroC  X   -0.09
ATOM  H18 Haro  X   0.14
ATOM  H17 Haro  X   0.14
ATOM  H16 Haro  X   0.14
ATOM  H15 Haro  X   0.14
ATOM  H14 Haro  X   0.14
```

```
ATOM  C17 aroC  X   -0.09
ATOM  C18 aroC  X   -0.09
ATOM  H8  Haro  X   0.14
ATOM  H7  Haro  X   0.14
ATOM  H20 Hapo  X   0.12
ATOM  H1  Haro  X   0.14
ATOM  H2  Haro  X   0.14
ATOM  O1  OH    X   -0.63
ATOM  O2  OH    X   -0.63
ATOM  H19 Hpol  X   0.46
BOND_TYPE  N1   C4  4
BOND_TYPE  N1  MN1  1
BOND_TYPE  N2   C6  4
BOND_TYPE  N2   C9  4
BOND_TYPE  N2  MN1  1
BOND_TYPE  N3   C11 4
BOND_TYPE  N3   C14 4
BOND_TYPE  N3  MN1  1
BOND_TYPE  N4   C16 4
BOND_TYPE  N4   C19 4
BOND_TYPE  N4  MN1  1
BOND_TYPE  N1   C1  4
BOND_TYPE  C1   C2  4
BOND_TYPE  C1   C20 1
BOND_TYPE  C2   C3  4
BOND_TYPE  C2   H1  1
BOND_TYPE  C3   C4  4
BOND_TYPE  C3   H2  1
BOND_TYPE  C4   C5  1
BOND_TYPE  C5   C6  1
BOND_TYPE  C5   C21 1
BOND_TYPE  C6   C7  4
BOND_TYPE  C7   C8  4
BOND_TYPE  C7   H3  1
BOND_TYPE  C8   C9  4
BOND_TYPE  C8   H4  1
BOND_TYPE  C9   C10 1
BOND_TYPE  C10  C11 1
BOND_TYPE  C10  H21 1
BOND_TYPE  C11  C12 4
BOND_TYPE  C12  C13 4
BOND_TYPE  C12  H5  1
BOND_TYPE  C13  C14 4
BOND_TYPE  C13  H6  1
BOND_TYPE  C14  C15 1
BOND_TYPE  C15  C16 1
BOND_TYPE  C15  C27 1
BOND_TYPE  C16  C17 4
BOND_TYPE  C17  C18 4
BOND_TYPE  C17  H7  1
BOND_TYPE  C18  C19 4
BOND_TYPE  C18  H8  1
BOND_TYPE  C19  C20 1
BOND_TYPE  C20  H20 1
BOND_TYPE  C21  C22 4
BOND_TYPE  C21  C26 4
```

```
BOND_TYPE  C22  C23 4
BOND_TYPE  C22  H9  1
BOND_TYPE  C23  C24 4
BOND_TYPE  C23  H10 1
BOND_TYPE  C24  C25 4
BOND_TYPE  C24  H11 1
BOND_TYPE  C25  C26 4
BOND_TYPE  C25  H12 1
BOND_TYPE  C26  H13 1
BOND_TYPE  C27  C28 4
BOND_TYPE  C27  C32 4
BOND_TYPE  C28  C29 4
BOND_TYPE  C28  H14 1
BOND_TYPE  C29  C30 4
BOND_TYPE  C29  H15 1
BOND_TYPE  C30  C31 4
BOND_TYPE  C30  H16 1
BOND_TYPE  C31  C32 4
BOND_TYPE  C31  H17 1
BOND_TYPE  C32  H18 1
BOND_TYPE  O1   O2  1
BOND_TYPE  O1  MN1  1
BOND_TYPE  O2   H19 1
CHI 1 MN1   O1   O2   H19
PROTON_CHI 1 SAMPLES 3 60 -60 180 EXTRA 1 20
CHI 2  N1  MN1   O1   O2
NBR_ATOM MN1
NBR_RADIUS 8.931877
ICOOR_INTERNAL   MN1    0.000000    0.000000    0.000000  MN1    N1    C4
ICOOR_INTERNAL    N1    0.000000  180.000000    2.087270  MN1    N1    C4
ICOOR_INTERNAL    C4    0.000000   56.371551    1.373193   N1   MN1    C4
ICOOR_INTERNAL    C3  177.515637   70.406629    1.455625   C4    N1   MN1
ICOOR_INTERNAL    C2    1.566661   73.855123    1.352559   C3    C4    N1
ICOOR_INTERNAL    C1   -1.124409   71.868814    1.445290   C2    C3    C4
ICOOR_INTERNAL    C20 177.768493   53.653166    1.409649   C1    C2    C3
ICOOR_INTERNAL    C19 -176.972013  53.601851    1.408434   C20   C1    C2
ICOOR_INTERNAL    N4    1.083169   54.192482    1.367587   C19   C20   C1
ICOOR_INTERNAL    C16  177.810908   72.947127    1.365121   N4    C19   C20
ICOOR_INTERNAL    C15 -177.881074   52.781644    1.403404   C16   N4    C19
ICOOR_INTERNAL    C14   -3.668112   55.332539    1.429093   C15   C16   N4
ICOOR_INTERNAL    N3    -1.328292   54.968584    1.371531   C14   C15   C16
ICOOR_INTERNAL    C11  174.146485   73.690913    1.359684   N3    C14   C15
ICOOR_INTERNAL    C10 -174.985056   54.560631    1.413397   C11   N3    C14
ICOOR_INTERNAL    C9    7.361486   54.379416    1.407308   C10   C11   N3
ICOOR_INTERNAL    N2    -5.895345   53.816935    1.371225   C9    C10   C11
ICOOR_INTERNAL    C6   179.581462   72.993366    1.369356   N2    C9    C10
ICOOR_INTERNAL    C5  -179.028343   53.919569    1.391479   C6    N2    C9
ICOOR_INTERNAL    C21 -176.808097   63.243911    1.505945   C5    C6    N2
ICOOR_INTERNAL    C22 -109.292716   57.740197    1.380440   C21   C5    C6
ICOOR_INTERNAL    C23  177.994407   58.900184    1.389221   C22   C21   C5
ICOOR_INTERNAL    C24    1.191699   60.561117    1.365270   C23   C22   C21
ICOOR_INTERNAL    C25   -1.052689   59.402041    1.387834   C24   C23   C22
ICOOR_INTERNAL    C26    0.188671   59.803462    1.387120   C25   C24   C23
ICOOR_INTERNAL    H13 -179.464897   59.703319    1.089155   C26   C25   C24
ICOOR_INTERNAL    H12 -179.995959   60.111137    1.091098   C25   C24   C26
ICOOR_INTERNAL    H11  179.870079   60.309783    1.090442   C24   C23   C25
```

```
ICOOR_INTERNAL    H10 -179.863327   59.722694    1.090177   C23   C22   C24
ICOOR_INTERNAL    H9   179.939547   60.498913    1.089810   C22   C21   C23
ICOOR_INTERNAL    C7   178.364013   71.095530    1.454731   C6    N2    C5
ICOOR_INTERNAL    C8     0.043108   72.453272    1.331036   C7    C6    N2
ICOOR_INTERNAL    H4  -179.481883   53.712913    1.089647   C8    C7    C6
ICOOR_INTERNAL    H3  -179.948925   53.798913    1.090006   C7    C6    C8
ICOOR_INTERNAL    H21 -179.987731   62.835262    1.031688   C10   C11   C9
ICOOR_INTERNAL    C12  176.490132   69.431136    1.438018   C11   N3    C10
ICOOR_INTERNAL    C13   -1.923524   73.061889    1.351686   C12   C11   N3
ICOOR_INTERNAL    H6  -178.574685   53.302880    1.090296   C13   C12   C11
ICOOR_INTERNAL    H5  -179.959190   53.505095    1.089966   C12   C11   C13
ICOOR_INTERNAL    C27  178.094564   62.178703    1.483561   C15   C16   C14
ICOOR_INTERNAL    C28  -54.182359   58.821963    1.399737   C27   C15   C16
ICOOR_INTERNAL    C29  178.735969   58.785946    1.400978   C28   C27   C15
ICOOR_INTERNAL    C30    1.067477   60.080629    1.378049   C29   C28   C27
ICOOR_INTERNAL    C31    1.105717   60.049092    1.384083   C30   C29   C28
ICOOR_INTERNAL    C32   -3.040842   60.753543    1.387997   C31   C30   C29
ICOOR_INTERNAL    H18 -176.930664   61.364413    1.089552   C32   C31   C30
ICOOR_INTERNAL    H17  179.905796   59.666518    1.089578   C31   C30   C32
ICOOR_INTERNAL    H16 -179.960940   60.032775    1.090250   C30   C29   C31
ICOOR_INTERNAL    H15 -179.977656   59.996812    1.089841   C29   C28   C30
ICOOR_INTERNAL    H14  179.966443   60.554384    1.089740   C28   C27   C29
ICOOR_INTERNAL    C17  179.549635   70.870565    1.464675   C16   N4    C15
ICOOR_INTERNAL    C18   -1.717415   73.609906    1.364694   C17   C16   N4
ICOOR_INTERNAL    H8  -178.970404   53.489861    1.089283   C18   C17   C16
ICOOR_INTERNAL    H7   179.922625   53.169359    1.089396   C17   C16   C18
ICOOR_INTERNAL    H20  179.999802   63.228920    1.032243   C20   C1    C19
ICOOR_INTERNAL    H1   179.969853   54.013494    1.090463   C2    C3    C1
ICOOR_INTERNAL    H2  -179.967048   53.093199    1.090850   C3    C4    C2
ICOOR_INTERNAL    O1   -87.313951   86.735033    1.771285  MN1    N1    C4
ICOOR_INTERNAL    O2   -88.797651   56.646661    1.251612   O1   MN1    N1
ICOOR_INTERNAL    H19  174.201993   74.629581    0.986709   O2    O1   MN1
```

References

1. Polizzi, N. F.; Wu, Y.; Lemmin, T.; Maxwell, A. M.; Zhang, S.-Q.; Rawson, J.; Beratan, D. N.; Therien, M. J.; DeGrado, W. F., De novo design of a hyperstable non-natural protein–ligand complex with sub-Å accuracy. *Nat. Chem.* **2017,** *9* (12), 1157-1164.
2. Zhou, J.; Grigoryan, G., Rapid search for tertiary fragments reveals protein sequence-structure relationships. *Protein Sci.* **2015,** *24* (4), 508-24.
3. Engel, D. E.; DeGrado, W. F., Alpha-alpha linking motifs and interhelical orientations. *Proteins* **2005,** *61* (2), 325-37.
4. Lahr, S. J.; Engel, D. E.; Stayrook, S. E.; Maglio, O.; North, B.; Geremia, S.; Lombardi, A.; DeGrado, W. F., Analysis and design of turns in alpha-helical hairpins. *J. Mol. Biol.* **2005,** *346* (5), 1441-54.
5. Bradley, P.; Misura, K. M.; Baker, D., Toward high-resolution de novo structure prediction for small proteins. *Science* **2005,** *309* (5742), 1868-71.
6. The PyMOL Molecular Graphics System, Version 2.0 Schrödinger, LLC.
7. Gassner, G. T., The styrene monooxygenase system. *Method. Enzymol.* **2019,** *620*, 423-453.
8. Otwinowski, Z.; Minor, W., Processing of X-ray diffraction data collected in oscillation mode. *Macromolecular Crystallography, Pt A* **1997,** *276*, 307-326.

9. Adams, P. D.; Afonine, P. V.; Bunkóczi, G.; Chen, V. B.; Davis, I. W.; Echols, N.; Headd, J. J.; Hung, L.-W.; Kapral, G. J.; Grosse-Kunstleve, R. W.; McCoy, A. J.; Moriarty, N. W.; Oeffner, R.; Read, R. J.; Richardson, D. C.; Richardson, J. S.; Terwilliger, T. C.; Zwart, P. H., PHENIX: a comprehensive Python-based system for macromolecular structure solution. *Acta crystallographica. Section D, Biological crystallography* **2010,** *66* (2), 213-221.
10. Emsley, P.; Cowtan, K., Coot: model-building tools for molecular graphics. *Acta crystallographica. Section D, Biological crystallography* **2004,** *60* (Pt 12 Pt 1), 2126-2132.